

See discussions, stats, and author profiles for this publication at: <https://www.researchgate.net/publication/10825402>

Theoretical Studies on the Inhibition Mechanism of Cyclooxygenase-2. Is There a Unique Recognition Site?

ARTICLE *in* JOURNAL OF MEDICINAL CHEMISTRY · MAY 2003

Impact Factor: 5.45 · DOI: 10.1021/jm0209376 · Source: PubMed

CITATIONS

42

READS

15

5 AUTHORS, INCLUDING:



Robert Soliva

University of Barcelona

18 PUBLICATIONS 545 CITATIONS

SEE PROFILE



Susana G Kalko

IDIBAPS August Pi i Sunyer Biomedical Resea...

67 PUBLICATIONS 1,041 CITATIONS

SEE PROFILE

Theoretical Studies on the Inhibition Mechanism of Cyclooxygenase-2. Is There a Unique Recognition Site?

Robert Soliva,^{†,‡} Carmen Almansa,[‡] Susana G. Kalko,[†] F. Javier Luque,^{*,§} and Modesto Orozco^{*,†}

Departament de Bioquímica i Biologia Molecular, Facultat de Química, Universitat de Barcelona, Martí i Franquès 1, Barcelona 08028, Spain, Molecular Modeling and Bioinformatics Unit, Institut de Recerca Biomèdica, Parc Científic de Barcelona, Josep Samitier 1-5, Barcelona 08028, Spain, Drug Discovery, J. Uriach i Cia, Camí Reial 51-57, Polígon Industrial Riera de Caldes, Palau de Plegamans, Barcelona 08184, Spain, and Departament de Fisicoquímica, Facultat de Farmàcia, Universitat de Barcelona, Avda Diagonal 643, Barcelona 08028, Spain

Received May 14, 2002

The mechanism of binding of different nonsteroidal anti-inflammatory drugs to the cyclooxygenase active site of cyclooxygenase-2 (COX-2) has been studied by means of a wide range of theoretical techniques including molecular dynamics and free energy calculations. It is found that theoretical methods predict accurately the binding of different drugs based on different scaffolds. Calculations allow us to describe in detail the key recognition sites and to analyze how these recognition sites change depending on the scaffold of the drug. It is concluded that the recognition site of COX-2 is very flexible and can adapt its structure to very subtle structural changes in the drug.

Introduction

Prostaglandins are ubiquitous endogenous lipids that play a key role in many physiological processes. Thus, they exert a cytoprotective action in the gastric mucosa and are crucial for normal renal function.¹ Moreover, it is well-known that prostaglandins trigger inflammation^{2–5} and the inhibition of their synthesis in the inflammatory site is one of the best mechanisms to control inflammation and its associated pain.^{2–8}

Nonsteroidal anti-inflammatory drugs (NSAIDs), a family including drugs such as aspirin, ibuprofen, and naproxen, exert their anti-inflammatory, analgesic, and antipyretic action by a mechanism that involves inhibition of the synthesis of prostaglandins.^{4–9} Particularly, they inhibit prostaglandin endoperoxide synthases, also known as cyclooxygenases (COXs), which catalyze the first two steps in the arachidonic acid cascade that generates prostaglandins from arachidonic acid. COXs catalyze first the cyclooxygenation of arachidonic acid, leading to prostaglandin G₂. This intermediate diffuses and enters into a second active site of the enzyme, which has peroxidase activity and catalyzes the conversion of prostaglandin G₂ into prostaglandin H₂.^{3,8}

For many years, both desired (anti-inflammatory) and undesired (ulcerogenic) effects of NSAIDs were attributed to inhibition of only one COX enzyme.^{5,6} In the early 1990s, two groups independently detected the existence of two cyclooxygenases:^{10–12} COX-1, which is present in most cells, and COX-2, which is expressed only in the central nervous system and in inflammatory

cells.^{3,7,8,13} After the discovery of these two isoforms, it became clear that the inhibition of COX-2 was responsible for the anti-inflammatory activity of traditional NSAIDs while the inhibition of COX-1 was involved in the ulcerogenic properties of these drugs.^{4,7–9,14} This opened the possibility of developing new NSAIDs designed to inhibit COX-2 but not COX-1, leading then to anti-inflammatory properties without undesirable side effects.^{7–9,15}

The first compound, DUP-697¹⁶ (see Figure 1), with a clear COX-2 specificity was developed in the early 1990s and served as a template for the development of new drugs, among them celecoxib^{17,18} and rofecoxib¹⁹ (see Figure 1). The last two molecules are in clinical use as anti-inflammatory and analgesic drugs free of ulcerogenic properties. The basis for their COX-2 specificity became evident once the 3D structures of COX-1 and COX-2 were solved.^{21,22} It was found that the change of two isoleucines (Ile523, Ile434) in COX-1 by two valines in COX-2 enlarged the NSAID-binding site around 25%, making accessible a hydrophobic pocket in COX-2 (but not COX-1).^{8,21,22} Aromatic groups of COX-2 specific NSAID drugs derived from DUP-697 occupy this pocket. Another key difference between COX-2 and COX-1⁸ is the mutation of His513 (COX-1) by Arg (COX-2). This substitution generates a specific binding site for sulfonamide or methylsulfone groups. The importance of this specific interaction becomes clear when we consider that almost all COX-2 specific drugs have a methylsulfone or sulfonamide group in a position that makes the interaction with Arg possible.^{7,8,23}

Besides the tremendous amount of experimental^{1–25} and theoretical^{26–32} work focused on the study of COX-2 and the existence of high-resolution structural information on the binding site of NSAIDs, several aspects of the binding mechanism of DUP-697-related compounds to COX-2 remain unclear. Inspection of experimental data^{7,8,18,24} reveals that empirical rules formulated for a given set of drugs are useless when applied to a

* To whom correspondence should be addressed. For M.O.: address, Molecular Modeling and Bioinformatics Unit, Institut de Recerca Biomèdica, Parc Científic de Barcelona, Josep Samitier 1-5, Barcelona 08028, Spain; phone, +34 93 4037156; fax, +34 93 4037157; e-mail, modesto@luz.bq.ub.es. For F.J.L.: phone, +34 93 4024557; fax, +34 93 4035987; e-mail, javier@far1.far.ub.es.

[†] Departament de Bioquímica i Biologia Molecular, Universitat de Barcelona, and Institut de Recerca Biomèdica.

[‡] Drug Discovery.

[§] Departament de Fisicoquímica, Universitat de Barcelona.

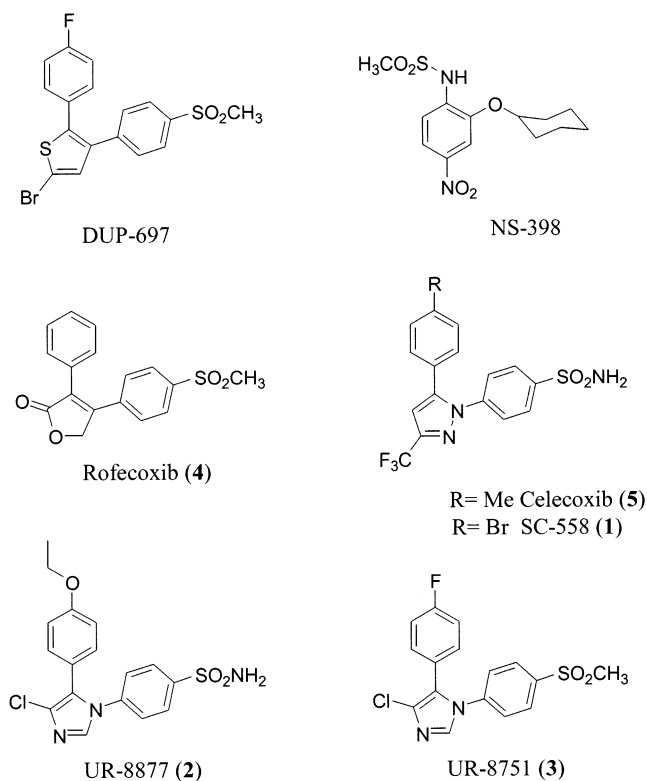


Figure 1. Structures of selective COX-2 inhibitors.

different set, even when both sets of compounds share a common backbone. This suggests that subtle structural changes in the binding site of COX-2 might occur to adapt its structure to the inhibitor.

In this paper a wide theoretical study on the mechanism of recognition of COX-2 specific NSAIDs based on DUP-697 topology is presented. The study combines fractional solvation calculations, classical molecular interaction potentials (cMIP), molecular dynamics (MD), and free energy calculations and represents, to our knowledge, one of the most systematic studies of drug–protein interactions in COX-2.

Methods

Molecular Interaction Analysis. To obtain a consensus pharmacophoric pattern of DUP-697-like compounds, reactivity analysis of different compounds based on celecoxib, rofecoxib, UR-8877, and UR-8751 cores were performed (see Figure 1). For this purpose, the atomic hydrophobicity parameters were computed by using our fractional AM1-MST model.³³ This method partitions the solvent response induced by the solute charge distribution into contributions associated with surface elements (ζ^s), which can then be combined to obtain the contribution of the surface around a given atom/group i to the solvation of the molecule (see ref 33 for details). The fractional hydrophobic parameters are then defined from the fractional parameters for solvation in water^{34,35} (ζ_{water}^s) and *n*-octanol³⁶ (ζ_{octanol}^s) using

$$\zeta_{\text{h}}^i = \sum_{s \in i} \zeta_{\text{water}}^s - \sum_{s' \in i} \zeta_{\text{octanol}}^{s'} \quad (1)$$

Finally, atomic/group contributions to hydrophobicity (ζ_{h}^i) are projected onto van der Waals surfaces to display the distribution of polar and apolar areas in the drugs.

The intrinsic ability of the active site to interact with small molecules was examined using our classical molecular interaction potential (cMIP) method,³⁷ where the protein is repre-

sented as a set of point charges with suitable van der Waals parameters and the solvent is treated as a continuum medium. For different configurations of the active site (obtained from crystal or MD data; see below), the interaction energy (eq 2) between the protein and different probes (O^- or O^+) was computed in a cubic grid around the active site of the protein by adding a Lennard-Jones term identical to that implemented in the AMBER force field (eq 3) to the solvent-screened electrostatic potential determined by solving the linear version of the Poisson equation (eq 4).^{37,38} Dielectric constants of 2 and 80 were assigned to the interior of the protein and to the solvent. AMBER-95³⁹ (parm94 file) force field and other suitable parameters (see below) were used to represent protein–drug interactions.

$$E_i^s = Q_s \Phi_i^{\text{ele}} + U_i^{\text{W},s} \quad (2)$$

where E_i^s stands for the interaction energy of the protein with the probe s placed at grid point i , Q_s is the charge of the probe, Φ_i^{ele} is the solvent-screened electrostatic potential at grid point i , and $U_i^{\text{W},s}$ is the van der Waals energy between the protein and the probe placed at grid point i .

$$U_i^{\text{W},s} = \sum_m (\epsilon_m \epsilon_s)^{1/2} \left[\left(\frac{r_m^* + r_s^*}{r_{mi}} \right)^{12} - 2 \left(\frac{r_m^* + r_s^*}{r_{mi}} \right)^6 \right] \quad (3)$$

where m denotes the atoms in the protein, r_x^* and ϵ_x are the van der Waals radius and hardness of atoms in the protein ($x = m$) or the probe ($x = s$), and r_{mi} is the distance from atom m to grid point i .

$$\nabla \cdot [\epsilon(r) \nabla \Phi^{\text{ele}}(r)] = -4\pi \rho_{\text{int}}(r) \quad (4)$$

where $\epsilon(r)$ is the dielectric permittivity, which depends on the position, and ρ_{int} denotes the charge distribution inside the boundary that separates protein and solvent.

Molecular Dynamics. The structure of human COX-2 was modeled from the crystal structure of murine COX-2 complexed to celecoxib analogue SC-558 (PDB entry 1cx2)²² by homology modeling and restrained molecular mechanics optimization. Owing to the position of the NSAID binding site, only one monomer, containing 556 residues, was considered in the calculations. The neutrality of the system was imposed by adding Na^+ and Cl^- ions. To this end, all charged groups without another oppositely charged residue located at less than 5 Å were neutralized by adding a suitable counterion, which was positioned by using the iterative protocol reported to set up MD simulations of proteins.³⁷ In this protocol, the best position for the counterion is determined from a cMIP calculation, and every time a new counterion is added, the total potential of the system (protein + counterions) is recomputed. The resulting neutral system was then hydrated by a sphere of water molecules centered at the NSAID binding site having a radius of 34 Å. A half harmonic potential was used to guarantee the integrity of the solvation sphere. The different simulation systems were constructed from this initial experimental model by replacing the initial ligand by the suitable drug.

The different starting models were optimized by using (i) 7000 cycles of energy minimization of water molecules, (ii) 2000 cycles of energy minimization of the entire system except the heme group and the drug, and (iii) 2000 cycles of energy minimization of the entire system except the drug. The optimized systems were then divided into a mobile and a frozen region. The first contained the inhibitor, all the waters, and the enzyme residues with at least 1 atom within 18 Å from the inhibitor, while the second included the rest of residues. The same systems were used for MD and MD/TI calculations.

The optimized systems were heated by increasing the temperature from 150 to 300 K in four steps during 80 ps. The thermalized systems were equilibrated for 100 ps and were used as a starting point for production MD runs of 1.5

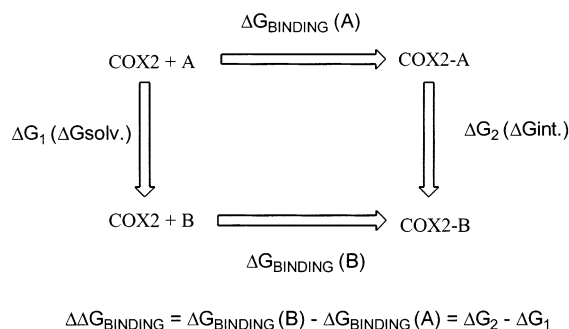


Figure 2. Thermodynamic cycle used to compute differences in free energy of binding between related inhibitors.

ns at constant temperature (300 K). SHAKE⁴⁰ was used to maintain all the bond lengths at their equilibrium value, in conjunction with a time step of 2 fs for integration of Newton equations. Shorter trajectories were performed to study specific details of protein–ligand interactions. A 14 Å cutoff was used for nonbonded interactions. Inspection of the trajectories confirmed the lack of charge discontinuities around the boundary of the 14 Å cutoff sphere. The size of the system and the unclear placement of the interface with the membrane preclude the use of a more accurate definition of the solvent environment.

AMBER-95 (parm94 file) and TIP3P force-fields^{39,41} were used for the protein residues and water molecules. The heme group was represented by using the parameters found in the AMBER web page.⁴² When necessary, force-field parameters for the inhibitors were developed. For this purpose, the compounds were optimized at the AM1 level,⁴³ and single-point HF/6-31G(d) calculations were performed to obtain molecular electrostatic potentials, which were used to obtain RESP-derived atomic charges.⁴⁴ Since van der Waals parameters are largely transferable, values for nonstandard functional groups were taken from the data compiled in the parm99 file (halogens, $r^* = 1.7500$ (F), 1.9480 (Cl), and 2.2200 (Br) Å; $\epsilon_r^* = 0.0610$ (F), 0.2650 (Cl), and 0.3200 (Br) kcal/mol) or adopted from related atoms in the parm94 file (for sulfone and sulfonamide groups, $r^* = 2.0000$ (S), 1.6612 (O), 1.8240 (N), 1.9080 (C), and 0.6000 (H) Å; $\epsilon_r = 0.2500$ (S), 0.2100 (O), 0.1700 (N), 0.0157 (C), and 0.1094 (H) kcal/mol). Equilibrium bond lengths and angles were taken from the AM1-optimized values, while stretching and bending force constants were transferred from the AMBER-95 (parm94 file) force field. Torsion parameters were parametrized from AM1 profiles using the PA-PQMD procedure,⁴⁵ which guarantees that the total AM1 and AMBER global torsional profiles were as close as possible for all the torsional angles studied. On the basis of our experience and taking into account the rigidity of the inhibitors, we did not consider necessary a more accurate parametrization based on ab initio calculations. Force-field parameters for all the inhibitors studied here are available upon request.

Free Energy Calculations. Thermodynamic integration (TI) calculations were carried out to determine the difference in binding free energy between two related inhibitors. Following standard thermodynamic cycles (see Figure 2), the mutation between inhibitors was performed by using 41 windows both in the complex with the protein and in water. Each window consisted of 5 (or 10) ps of equilibration and 5 (or 10) ps of averaging for a total of 410 (820) ps of MD simulation for each mutation in the bound (protein) or unbound (water) states. The mutations for the bound state of the inhibitors were performed using the equilibrated structures obtained at the end of the 1.5 ns MD simulation. The mutations of the inhibitors in water were performed in cubic systems containing the inhibitor and around a thousand waters, which were previously equilibrated in the *NPT* ensemble (1 atm, 300 K) using periodic boundary conditions, an integration step of 2 fs, SHAKE, and a 14 Å residue-based cutoff. Technical details of the trajectories used in TI calculations were identical to those used in MD simulations (see above). Final free energy

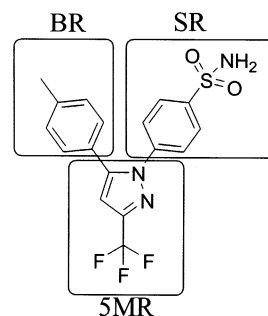


Figure 3. Regions in which inhibitors are divided for discussion purposes.

values and their error were obtained by averaging the results for the first and second halves of the 410 and 820 ps simulations (i.e., each value reported here is based on four independent free energy estimates).

Analysis of Key Residues for Drug–Protein Recognition. To analyze which residues of the protein were more relevant for interaction with the drugs, different MD trajectories were analyzed using UBEXTRACT,⁴⁶ a locally developed program that computes MD-averaged interaction energies between the drugs (or parts of them) and the protein (eq 5). The interaction energy is expressed as the addition of electrostatic (E_{ele}) and van der Waals (E_{vw}) terms (eq 5). The electrostatic energy between point charges in the protein (Q_m) and the ligand (Q_l) is evaluated by using a Coulombic expression (eq 6) in conjunction with a distance-dependent dielectric constant ($\epsilon(r_{ml})$, eq 7), which was developed on the basis of dissociation data of organic acids and bases and validated by comparison against finite difference Poisson–Boltzmann calculations.⁴⁷ The van der Waals term is evaluated by using a Lennard-Jones expression identical to that implemented in the AMBER force field (eq 4). The charges and van der Waals parameters used in MD simulations were also considered in UBEXTRACT computations. Because of the averaging along the trajectories, UBEXTRACT results are mostly free of statistical noise, allowing us to identify very quickly and with noticeable accuracy the most relevant residues for the drug–protein interaction.

$$E_{\text{UBEXTRACT}} = \langle E_{\text{ele}} + E_{\text{vw}} \rangle_{\text{MD}} \quad (5)$$

$$E_{\text{ele}} = \sum_{m,l} \frac{Q_m Q_l}{\epsilon(r_{ml}) r_{ml}} \quad (6)$$

$$\epsilon(r_{ml}) = A + \frac{\epsilon_0 - A}{1 + B \exp(-C(\epsilon_0 - A)r_{ml})} \quad (7)$$

where $A = -8.5525$, $B = 7.7839$, $C = 0.003627$, and ϵ_0 is the dielectric constant of water.

Results and Discussion

Three structural moieties can be identified in the drugs under study (see Figure 3): (i) the central five-membered ring (5MR), (ii) the sulfone/sulfonamide substituted benzene (SR), and (iii) the other substituted or unsubstituted benzene residue (BR). All the drugs are mostly hydrophobic, as noted in the blue surfaces shown in Figure 4. However, there are subtle differences between the drugs and between parts of the drugs. The SR moiety is clearly amphipathic, with a highly polar sulfone/sulfonamide group in the para position of an apolar benzene ring. The BR moiety is fully apolar for all the compounds, suggesting a common apolar binding pocket for this region of the drug. Finally, the 5MR subunit is fully apolar for some of the compounds, while

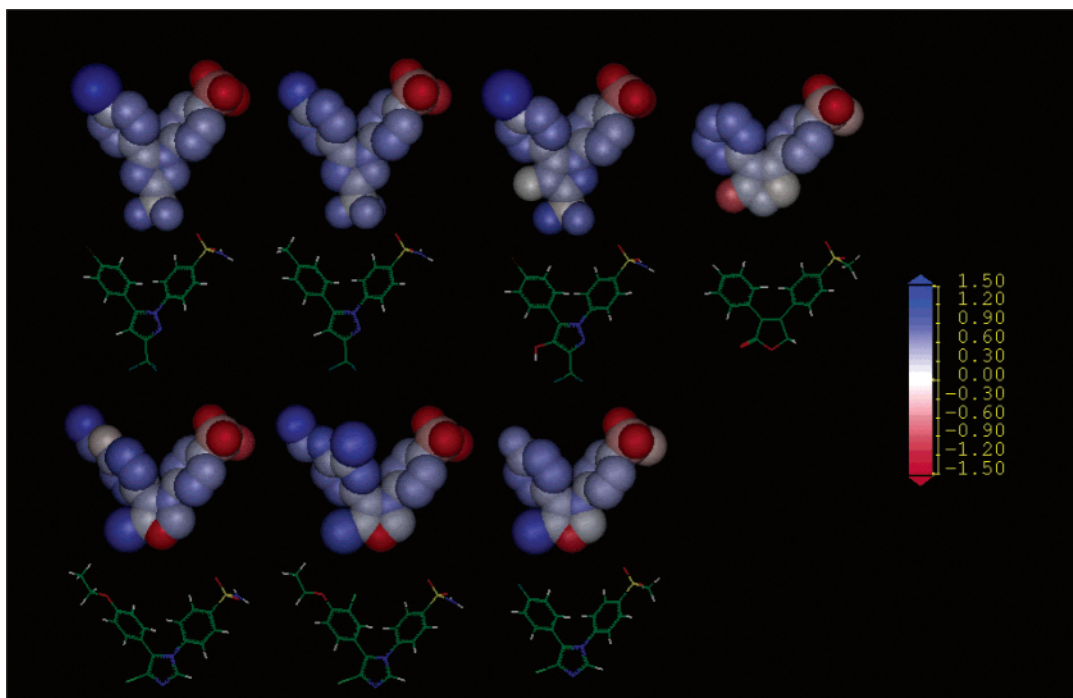


Figure 4. Fractional hydration plots of different inhibitors of COX2. Code color (in kcal/mol) is shown at right (blue surfaces mean preferential solvation in *n*-octanol, and red surfaces mean preferential solvation in water). Compounds (from top left to bottom right) are **1**, **5** (celecoxib), **7**, **4**, **2**, **11**, and **3**.

it is partially polar for others, suggesting that dual binding modes might be involved for this part of the molecule.

Celecoxib Binding Mode. According to the crystal structure of COX-2 with the celecoxib analogue SC-558, the active site is mostly hydrophobic (10 highly apolar residues and only 2 charged groups) and most of the drug–protein contacts are stabilized by van der Waals interactions. The 5MR moiety is surrounded (at less than 5 Å) by Val116, Arg120, Val349, Ser353, Tyr355, Leu359, and Ala527, defining a hydrophobic site, where only Arg120 (placed near the CF₃ group) introduces a strong electrostatic field. The SR group is near His89, Asn192, Leu352 (also close to BR), Arg513, Ala516, Ile517, Phe518, and Val523. Finally, the BR group is surrounded by Tyr348, Phe381, Leu384, Tyr385, Trp387, Gly526, Ala527 (also close to 5MR), and Ser530.

The crystal structure of COX-2 bound to the celecoxib analogue (pdb entry 1cx2; solved to 2.5 Å resolution) was used as a starting model for our simulations. Inspection of the structure, however, revealed a mistake in the positioning of the sulfonamide group with respect to Arg513. As noted by others,²⁸ its location in the crystal is not consistent with a tight binding of the drug, since a bad N–N contact between sulfonamide and guanidinium groups is found. MD simulations and energy analysis revealed that an alternative conformation of the sulfonamide group is preferred. In such a conformation, which is fully consistent with the electron density map, one oxygen group of the sulfonamide moiety is hydrogen-bonded to Arg513, thus removing the bad N–N contact.

A 1.5 ns MD trajectory allows us to obtain an average view of the enzyme active site bound to celecoxib. As expected, no major changes from the reported X-ray structure are found during the MD trajectory except for (i) the rotation of the sulfonamide group to generate a

favorable N(+)-O(sulfonamide) interaction (average N–O distance of 3.2 Å and average N–H–O angle of 160°) and (ii) the conformational change of the side chain of Ser 530 to form first a H bond with Gly526 and later in the trajectory to form a water-mediated hydrogen bond with Tyr385, as found by Jorgensen's group from Monte Carlo simulations.²⁸

CMIP calculations (see Figure 5) show a very clear Y-shaped van der Waals contour that fits well the structure of celecoxib. Besides a local free accessible volume on the BR side of 5MR, there is no more empty space, suggesting that no large increases in size or shape of the inhibitor can be tolerated by the enzyme. There are small regions of favorable interaction with O⁺, the most important one corresponding to the sulfonamide binding site. Finally, there are regions of favorable interaction with O[−] located around Arg120 (near the region where the CF₃ group of the 5MR is located) and also a smaller one around Ser530 and Tyr385, i.e., the position where a water molecule bridging Ser530 and Tyr385 is located during large periods of the trajectory.

The UBEXTRACT analysis shows that only a few residues of the protein make important interactions with the drug (see Figure 6). In fact, no residues are found to form, on average, unfavorable interactions. As expected from the hydrophobicity of the drugs and the cMIP analysis (see above), most of the interactions stem from dispersion, as noted in the large stabilizing value of the van der Waals contributions. In fact, whereas only four residues (Arg120 (with 5MR), Asn192 (SR), Leu352 (SR), and Arg513 (SR)) show significant electrostatic interactions with the drug, 13 residues participate in strong van der Waals contacts, particularly 5MR with Val349, Ser353, and Tyr355; SR with Phe518 and Val527; and BR with Ala527. Additional weaker contacts with other residues are also found (see Figure 6). Interestingly, most of the interactions involve both 5MR

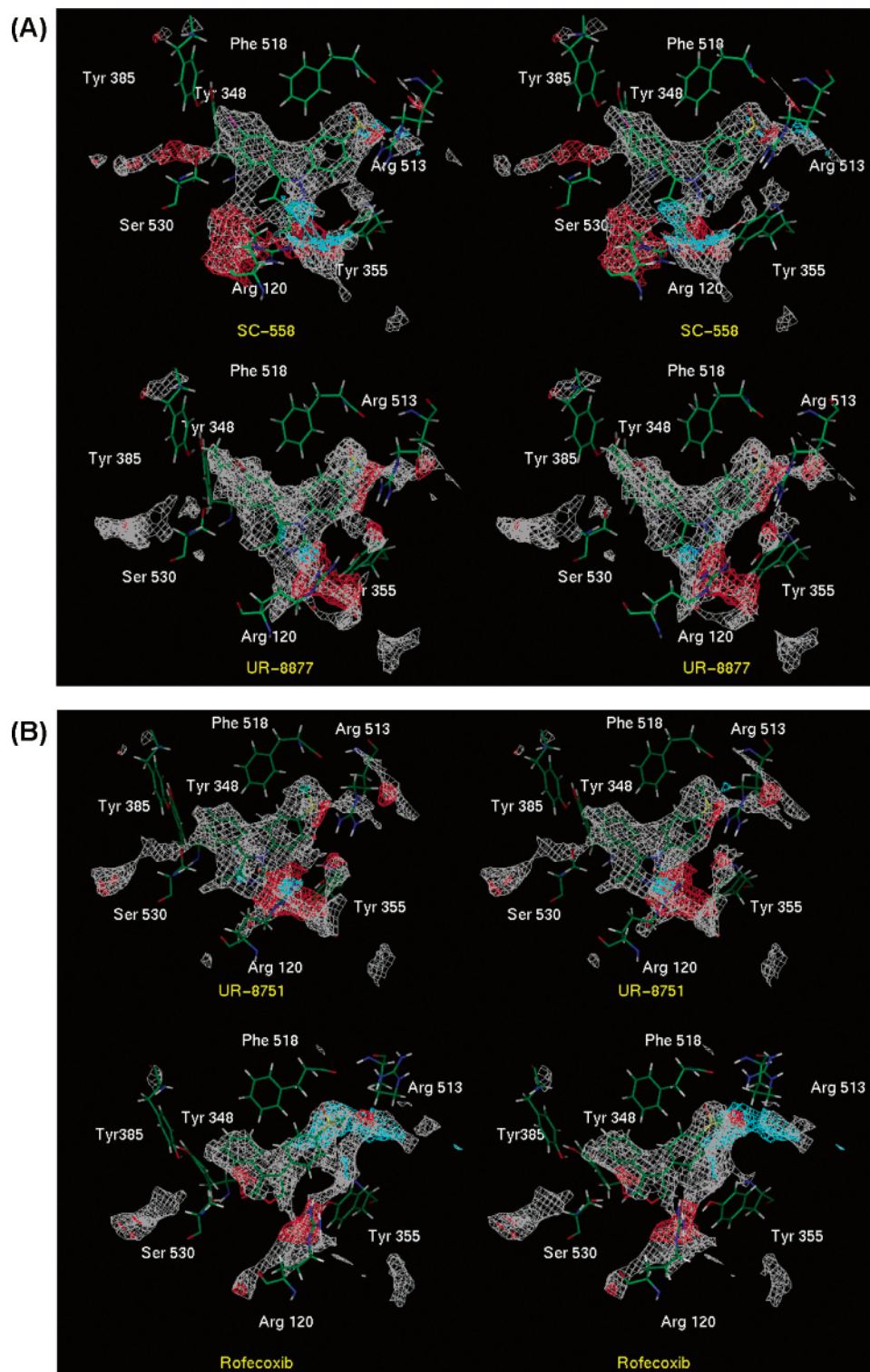


Figure 5. CMIP stereoplots for the active site of COX-2 when bound to different inhibitors: (A) (top) celecoxib analogue **1** (SC-558) and (bottom) UR-8877 (compound **2**); (B) (top) UR-8751 (compound **3**) and (bottom) rofecoxib (compound **4**). CMIP calculations have been performed using a neutral carbon (white contour, -1.5 kcal/mol), an O $^-$ (red contour, -6 kcal/mol), and an O $^+$ (blue contour, -6 kcal/mol).

and SR units, while the BR group seems to be less tightly bound to the enzyme. This finding agrees with the fact that 5MR and SR moieties accept less structural modifications than the BR subunit.

To determine whether the binding mode found is useful for predicting the differential binding affinity of celecoxib derivatives, the changes in binding free energy due to chemical changes in 5MR and BR units were

estimated from MD/TI simulations. Results are given in Table 1 (see also Figure 7), which also reports experimental values estimated from IC_{50} data (see eq 8; since the substrate concentration in the pharmacological assays was the same for all the competitive reversible inhibitors, the differences in binding free energies were derived by exploiting the relationship $IC_{50} = K_i(1 + [S]/K_m)$, where K_m and K_i are Michaelis and

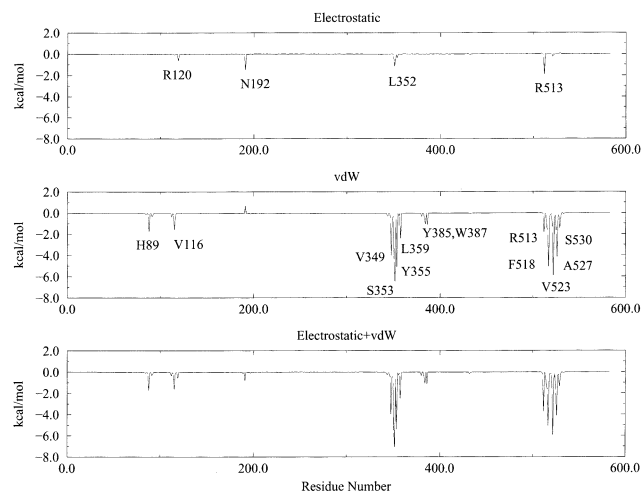


Figure 6. UBEXTRACT plots (electrostatic, van der Waals, and total energy) for the interaction of SC-558 with the different residues of the protein (values shown correspond to the average of 1.5 ns of MD simulation).

Table 1. Changes in Binding Free Energy (kcal/mol) Associated with Different Chemical Modifications of the Celecoxib Derivative SC-558 (Compound **1**), UR-8877 (Compound **2**), UR-8751 (Compound **3**), and Rofecoxib (Compound **4**)^a

mutation	$\Delta\Delta G^{\text{int}}$	$\Delta\Delta G^{\text{solv}}$	$\Delta\Delta G^{\text{tot}}$	$\Delta\Delta G^{\text{exp}}$
1 → 5	−0.1(0.0)	−0.2(0.1)	0.1(0.1)	0.8
1 → 6	1.6(0.1)	−1.0(0.1)	2.6(0.1)	4.4
1 → 7	−1.9(0.1)	−4.9(0.1)	3.0(0.1)	3.0
1 → 8	−0.8(0.0)	−1.5(0.2)	0.7(0.2)	0.7
1 → 9	2.4(0.2)	−1.9(0.2)	4.3(0.3)	≥4.7
2 → 10	0.9(0.1)	−1.0(0.1)	1.9(0.1)	2.8
2 → 11	0.4(0.0)	0.7(0.1)	−0.3(0.1)	−0.4
3 → 12	3.6(0.2)	1.0(0.0)	2.6(0.2)	3.5
4 → 13	2.1(0.0)	1.8(0.2)	0.3(0.2)	~0
4 → 14	1.0(0.1)	−0.8(0.0)	1.8(0.1)	“inactive”

^a The differences in binding free energy determined from MD/TI simulations are divided ($\Delta\Delta G^{\text{tot}} = \Delta\Delta G^{\text{int}} - \Delta\Delta G^{\text{solv}}$) into interaction ($\Delta\Delta G^{\text{int}}$) and solvation ($\Delta\Delta G^{\text{solv}}$) terms. Theoretical values are compared with experimental estimates ($\Delta\Delta G^{\text{exp}}$) derived from IC₅₀ data (for the rofecoxib series, only qualitative values were reported in available experimental studies). Standard error in free energy values are in parentheses. See Figure 7 for structures.

enzyme–inhibitor dissociation constants).¹⁸ Theoretical and experimental values for the $\Delta\Delta G$ of binding for celecoxib derivatives agree well (Table 1). This agreement, and the small statistical uncertainties in the average free energy values displayed in Table 1, demonstrates not only the power of MD/TI calculations to reproduce relative binding free energies but also supports the binding mode for celecoxib derived after MD refinement of the crystal structure.

$$\Delta\Delta G_{\text{binding}}^{\text{A-B}} = RT \ln(\text{IC}_{50}^{\text{A}}/\text{IC}_{50}^{\text{B}}) \quad (8)$$

Further insight into the key interactions that mediate the binding of celecoxib to COX-2 can be gained from the results in Table 1. The presence of the CF₃ group in 5MR is crucial for the binding, as noted in the dramatic reduction of binding affinity found (both theoretically and experimentally) upon replacement of −CF₃ (**1**) by −CH₃ (**6**) or −H (**9**) groups. The difference in binding affinity can be explained by two factors: (i) the CF₃ group reduces the desolvation of the molecule upon binding ($\Delta\Delta G^{\text{solv}}$ in Table 1) and (ii) the CF₃ group

largely increases the magnitude of drug–protein interactions ($\Delta\Delta G^{\text{int}}$ in Table 1). To investigate why the presence of CF₃ in 5MR improves the drug–protein interaction, short MD trajectories (100 ps equilibration + 400 ps collection) were performed for COX-2 bound to compounds **1**, **6**, and **9**. The results (see Figure 8) confirmed the enthalpic nature of the stabilization induced by the −CF₃ group. Both electrostatic (with Arg513, Arg120, and Asn192) and van der Waals interactions (mostly with the hydrophobic pocket defined by Val349, Leu352, Tyr355, and Leu359) contribute to the preferential binding of the CF₃ group.

Results in Table 1 also point out that the introduction of a polar group on the BR side of 5MR (see Figure 3) decreases the binding free energy of SC-558 (**1** → **7**). Clearly, this is related to the increase in the desolvation penalty as a consequence of the presence of a polar group (−4.9 kcal/mol from results in Table 1 and Figure 7). Such a penalty is not fully compensated ($\Delta\Delta G^{\text{int}} = -1.9$ kcal/mol) by polar interactions between the hydroxyl in **7** and polar groups of the protein (mostly the carbonyl of Ala527), in agreement with the fact that the BR side of 5MR is located in a hydrophobic region of the active site.

UR-8877 and UR-8751 Binding Mode. The binding mode of chlorimidazoles **2** and **3** was explored from MD simulations using the crystal structure of COX-2 bound to the celecoxib analogue as the starting point for the trajectories. The equilibrated structure of the COX-2 active site when bound to UR compounds is not dramatically different from that found for celecoxib derivatives. The most important difference is a small rotation of the side chain of Arg120, which displaces the region of favorable interaction with the O[−] probe. Indeed, Ser530 adopts an “up” position and is hydrogen-bonded to the backbone of Gly526. This conformational change annihilates the region of favorable interaction with O[−] in the vicinities of Ser530, which was occupied by a water molecule in the COX-2-SC-558 complex.

UBEXTRACT interaction profiles for **2** and **3** are qualitatively similar to those obtained for celecoxib analogues, which indicates that a similar pattern of interactions mediates the binding of these compounds. However, the change from pyrazole to imidazole leads to local differences (see Figure 9) and leads to the loss of van der Waals contacts with Val116, Tyr355, Ser353, Val349, and Leu359. There is also a slight improvement in van der Waals contacts of the BR region with Phe381, Tyr385, and Trp387 and a slight decrease in favorable interactions of SR with Arg513. It is worth noting the small changes in the interaction profiles for **2** and **3**, which suggest that the differences in the binding mode of celecoxib and imidazole derivatives are not an artifact of molecular dynamics but a consequence of the structural changes between those compounds.

MD/TI free energy calculations reproduce well the changes in binding free energy associated with the attachment of substituents to the core of **2** and **3** (see Table 1), even in cases where chemical modifications improve (like the introduction of −Cl in the meta position of BR; mutation **2** → **11**) or sharply decrease (like the insertion of a Me group in the SR side of 5MR; mutation **3** → **12**) the activity. These results support

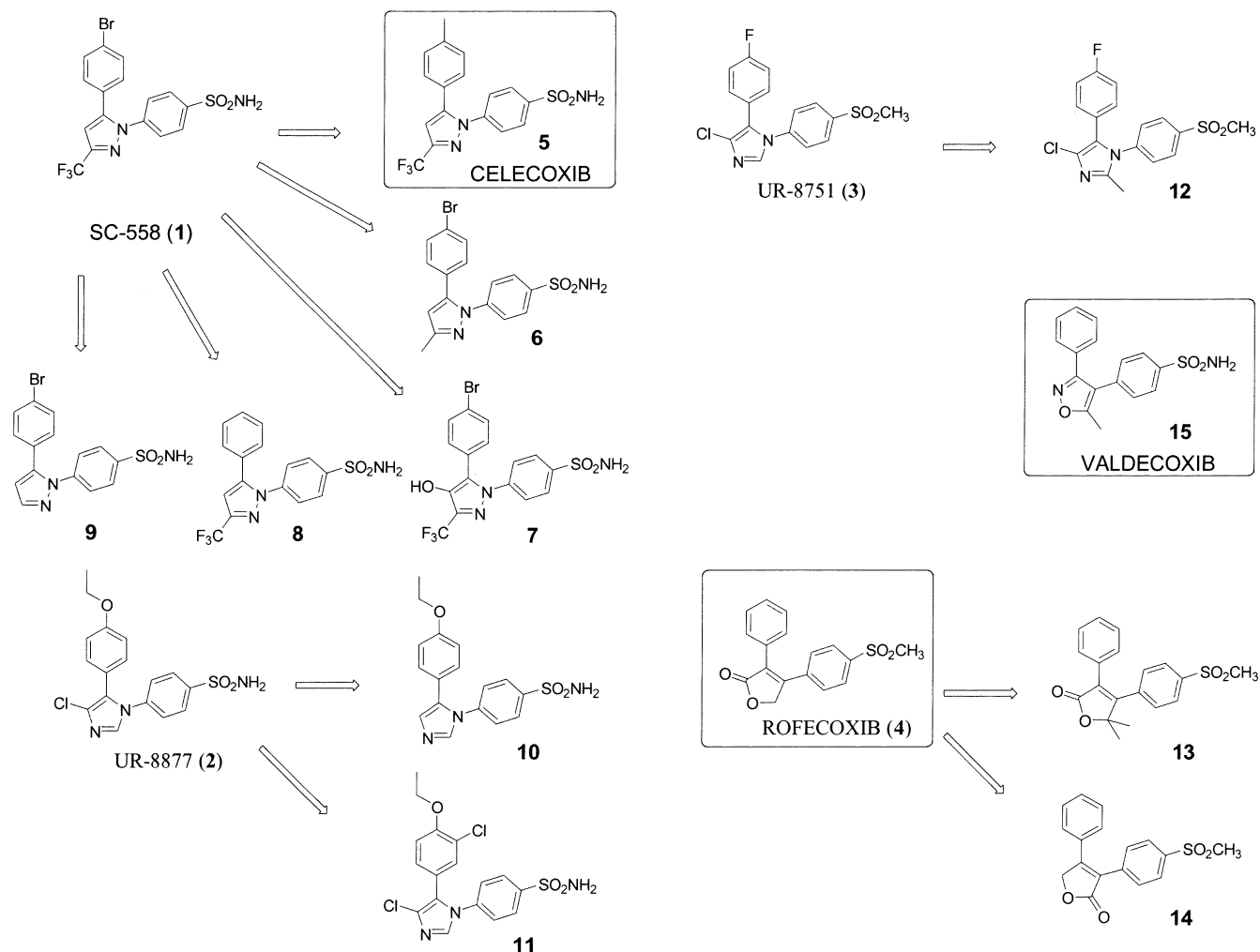


Figure 7. Summary of MD/TI calculations performed on the four lead compounds used in this study: SC-558 (compound 1), UR-8877 (compound 2), UR-8751 (compound 3), and rofecoxib (compound 4). The three marketed compounds are each enclosed in a rectangle.

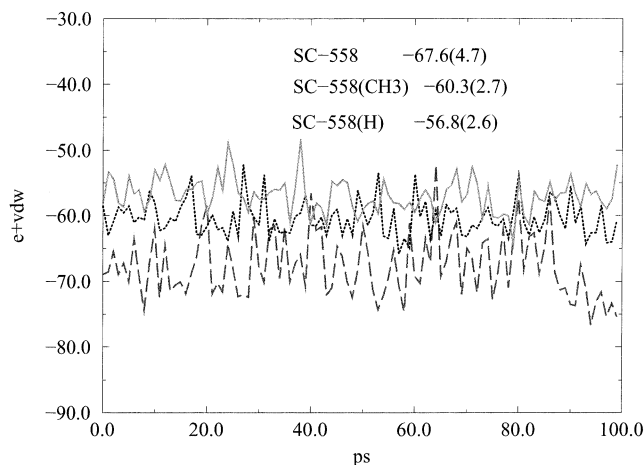


Figure 8. Differential interaction energy between COX-2 and compound 1 (long dashed line), compound 6 (SC-558-(CH₃), dotted line), and compound 9 (SC-558-(H), solid line).

the goodness of the proposed binding mode for these compounds.

Analysis of both theoretical and experimental data in Table 1 warns against the use of knowledge-based rules derived from the behavior of related series of molecules. Thus, inspection of experimental data for

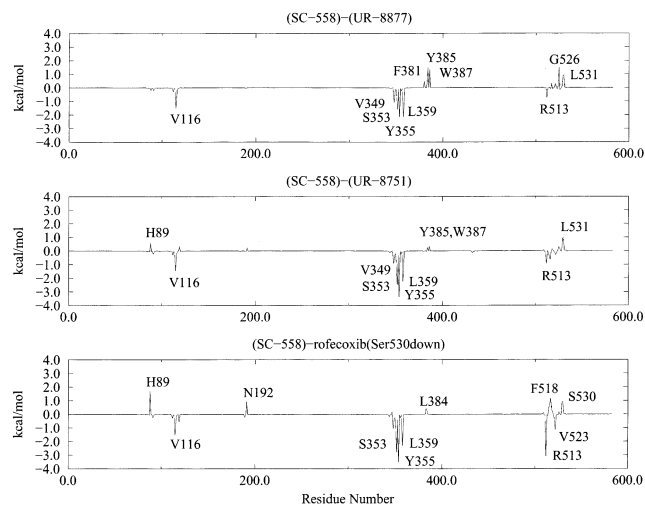


Figure 9. Differential UBEXTRACT plots for the four inhibitors considered here as lead compounds (the celecoxib analogue 1 is used as reference for all the calculations).

valdecoxib 15, a recently marketed COX-2 inhibitor,²⁵ suggests that a methyl group on the SR side of 5MR is favorable for binding, but the same substitution decreases drastically the binding of 3 (by around 3 kcal/mol). This suggests that subtle local rearrangements can

occur at the active site depending on the chemical nature of the compound, which can lead to important alterations of the pharmacophore (see below).

Rofecoxib Binding Mode. Though the general topology of rofecoxib **4** is similar to that of celecoxib **5**, non-negligible differences exist in the reactivity pattern of these two molecules, as noted in the hydrophobicity pattern (see above). This suggests that the binding mode of rofecoxib might not be similar to that of celecoxib. In fact, substitution of SC-558 by rofecoxib in a MD-equilibrated structure of the COX-2-SC-558 complex leads to stable trajectories (on the nanosecond time scale) with apparently good drug–protein interactions. Unfortunately, by use of this binding mode, different MD/TI calculations failed to predict the relative binding affinities between rofecoxib and compound **14** (a derivative where the lactone carbonyl moves from the BR to the SR side of 5MR). Thus, MD/TI calculations performed using different starting structures and simulation protocols suggested that **14** should bind 3–4 kcal/mol stronger than rofecoxib, in disagreement with qualitative experimental data.²⁴

The theoretical result is in fact not surprising and agrees with chemical intuition and with available binding data for other compounds. Thus, all data in the celecoxib series (see above) suggest that a polar group on the BR side of 5MR is disfavored because of the hydrophobicity of the binding site. Accordingly, compound **14** should bind COX-2 better than rofecoxib (as predicted by MD/TI calculations) because in the former the carbonyl oxygen is exposed to the solvent but in the latter (assuming it adopts the celecoxib binding mode) it fits an unfavorable apolar environment. In summary, the discrepancy between experimental and MD/TI calculations stems from the fact that the binding modes of rofecoxib and celecoxib are different and that the MD simulation (starting from the celecoxib binding mode) is not able to capture the transition to the rofecoxib binding mode.

The different binding mode of rofecoxib and celecoxib might imply that (i) the drugs fit different binding sites or that (ii) the binding site is the same, but there are local rearrangements that alter the interaction pattern. Docking studies with AUTODOCK⁴⁸ and cMIP³⁷ failed to detect alternative binding modes maintaining the requirement of the sulfone/sulfonamide binding site. On the basis of these studies as well as on the similar shape of rofecoxib and celecoxib, it is reasonable to assume that local rearrangements at the common binding site modify the drug–protein recognition pattern of the two drugs.

Compared to compound **14**, the larger binding affinity of rofecoxib suggests that the carbonyl group at the BR side of 5MR likely participates in hydrogen bonding. Inspection of the active site suggests that Ser530 is the only residue that can form such a hydrogen bond. Therefore, we analyzed three possible hydrogen-bond contacts: (i) a single water-mediated hydrogen bond, (ii) a double water bridge, and (iii) a direct H bond. MD/TI calculations with the first two models failed to reproduce the difference in binding free energy between rofecoxib and compound **14** and led to systems that should be entropically disfavored. Accordingly, the binding of rofecoxib should involve a direct hydrogen bond between

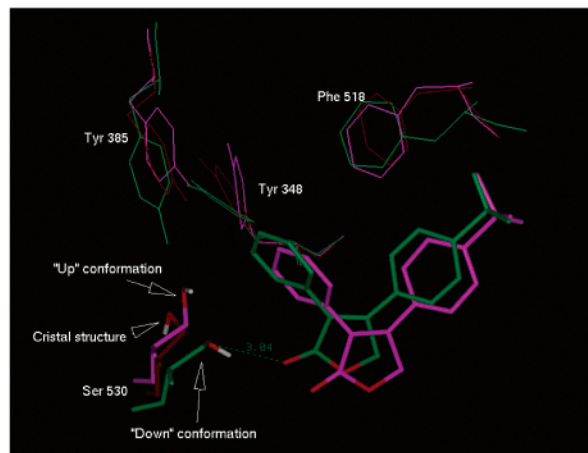


Figure 10. Details of the rofecoxib binding site when Ser530 is in the “up” (magenta) and in the “down” (green) conformation. The conformation found the crystal structure (brown) is also displayed for comparison.

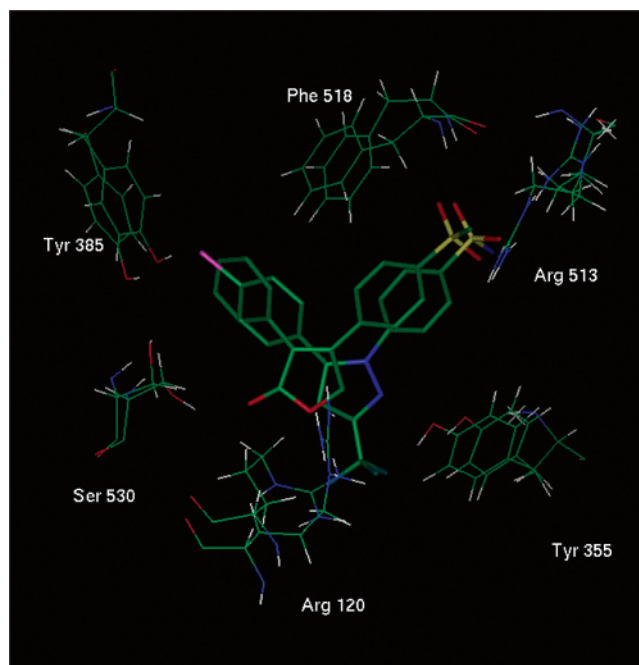


Figure 11. Comparison of the SC-558 and rofecoxib binding modes after superposition of both protein binding sites.

Ser530 and the carbonyl group of the drug. To achieve this contact, the side chain of Ser530 must adopt a “down” orientation (see Figure 10). Though the “up” conformation is favored by celecoxib because of water-mediated hydrogen bonds between Ser530 and Tyr385, a subtle displacement of rofecoxib with respect to celecoxib in the binding site (see Figure 11) makes possible the rotation of the side chain of Ser530 to the “down” conformation. In fact, the “down” conformation is slightly preferred for rofecoxib, as noted in Figure 12, which shows the energy of the active-site subsystem (the residues at the active site plus the inhibitor) for both the “up” and “down” conformations.

Inspection of the crystal structure of COX-2 suggests that the transition “up” → “down” should not be very difficult, since Ser530 seems to be in an intermediate conformation in the crystal (see Figure 10). However, MD simulations do not capture spontaneously this

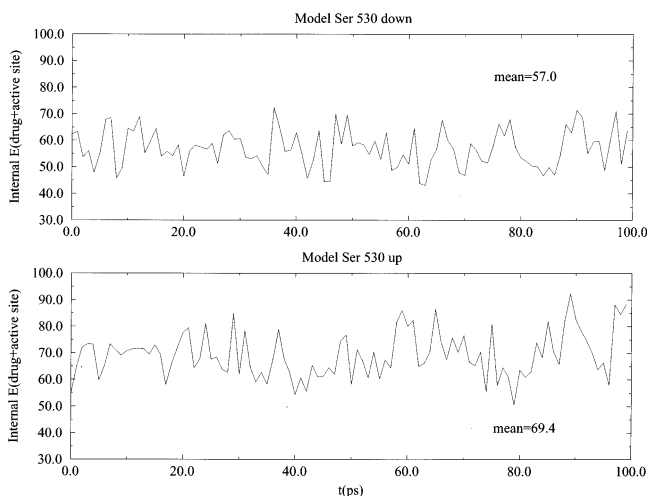


Figure 12. Active site energy for the COX-2-rofecoxib complex with Ser530 in the “up” and Ser530 in the “down” conformation. Active site energy is defined as the addition of the drug–protein interaction energy and the intra- and intermolecular energy of residues at the active site.

transition, which stresses the limitations of current simulation protocols to detect infrequent conformational transitions and points out the need to verify in all the cases the quality of MD sampling by direct comparison with functional experimental data. Manual rotation of the Ser530 side chain followed by molecular mechanics optimization and MD simulations (without restrictions in the Ser530 side chain) allowed us to sample structures of the COX-2 active site bound to rofecoxib with the Ser530 side chain in the “down” conformation. MD/TI simulations of the relative binding affinity of rofecoxib and compound **14** performed using the “down” conformation of Ser530 lead to a differential free energy of around 2 kcal/mol (see Figure 7 and Table 1), which agrees with qualitative experimental data.²⁴

The CMIP analysis of the rofecoxib binding site (Figure 5) shows that while the contour for the van der Waals probe is similar to that found for celecoxib and rofecoxib, the contours for the polar probes change significantly. Both the displacement of rofecoxib from the position occupied by celecoxib and the change from sulfonamide to methylsulfone shifts the location of the side chain of Arg513, which opens a region of more favorable interaction with a positive probe around the original position of the guanidinium group. The rotation of the Ser530 side chain leads to a region of favorable interaction with a negative probe, located close to the position of the carbonyl group of rofecoxib. Finally there is a displacement of the Arg120 side chain, which changes the region of favorable interaction with the O–probe. Interestingly, the same changes were found for UR compounds, as expected from the similar chemical environments at the bottom of 5MR in UR compounds and rofecoxib. In contrast, the lack of heteroatom lone pairs (O: in rofecoxib or N: in UR compounds) and the presence of the apolar CF₃ group determine a very different chemical environment (see Figure 3) for celecoxib.

Further information about the changes in the drug–protein interactions between celecoxib and rofecoxib is gained from UBEXTRACT analysis (see Figure 9). There is a loss of favorable van der Waals interactions

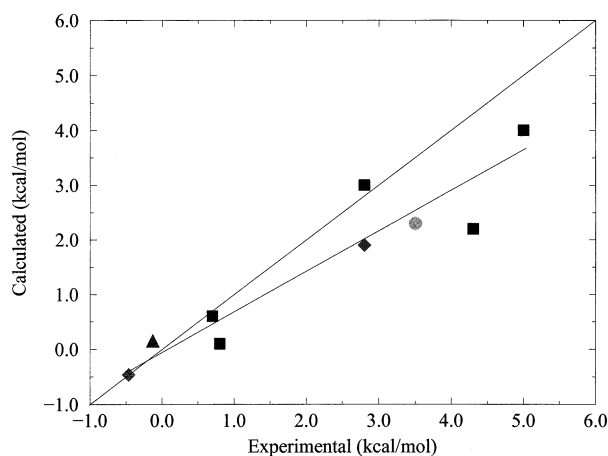


Figure 13. $\Delta\Delta G$ relative to inhibitors, a comparison of experimental and theoretical differential binding free energies for the four series of compounds studied here (square, mutations on SC-558; dot, mutations on UR-8751; triangle, mutations on rofecoxib; diamonds, mutations on UR-8877). The optimum regression line is $y = 0.73x$ (the error of the slope is 0.15), and the variance explained by the regression model amounts to 0.89. The ideal regression line ($y = x$) is also indicated as reference.

in the region of 5MR (especially Val116, Ser353, Tyr355, and Leu359). The changes in the SR region are more complex, since the loss of favorable electrostatic interactions with Arg513 is mostly compensated by better electrostatic interactions with His89 and Asn192. In summary, both UBEXTRACT and CMIP calculations point out that there are important changes in the pattern of key drug–protein interactions between celecoxib and rofecoxib. Once again, the rearrangements found during the dynamics appear to be related to structural changes of the drugs and not to spurious behavior of the MD simulations.

Conclusions

The study reported here shows the unique characteristics of the COX-2 binding site. In COX-2 inhibitors related to DUP-697, it has been shown that depending on the nature of the 5MR unit, local rearrangements in the binding site are possible, which can modify the pattern of drug–protein interactions. According to our simulations, different patterns are possible, leading to slightly different pharmacophores for COX-2 inhibitors. Caution is then necessary in SAR analysis, since knowledge-based rules derived from the analysis of a set of compounds can fail to describe the behavior of a related series of molecules. Despite the limitations of current simulation protocols, our results point out the power of MD and MD/TI simulations to reproduce quantitatively experimental binding data (see Figure 13) without a previous parametrization of the method, as others have recently shown.^{28,49} Furthermore, the combination of MD simulation with analysis techniques such as fractional analysis, UBEXTRACT, and cMIP methods seems very powerful for describing in detail complex patterns of interactions.

Acknowledgment. We thank Drs. Xavier Bartrolí, Federico Gago, and Juan Jesús Perez for valuable comments. This work has been supported by the Spanish Ministry of Science and Technology (Grants PB98-

1222 and PM99-0046). We also thank the Centre de Supercomputació de Catalunya (CESCA) for computational facilities.

References

- Dubois, R. N.; Abramson, S. B.; Crofford, L.; Gupta, R. A.; Simon, L. S.; van de Pute, L. B.; Lipsky, P. E. Cyclooxygenase in Biology and Disease. *FASEB J.* **1998**, *12*, 1063–1073.
- Portanova, J. P.; Zhang, Y.; Anderson, G. D.; Hauser, S. D.; Masferrer, J. L.; Seibert, K.; Gregory, S. A.; Isakson, P. C. Selective Neutralization of Prostaglandin E2 Blocks Inflammation, Hyperalgesia, and Interleukin 6 Production in Vivo. *J. Exp. Med.* **1996**, *184*, 883–891.
- Smith, W. L.; Garavito, R. M.; DeWitt, D. L. Prostaglandin Endoperoxide H Synthases (Cyclooxygenases)-1 and -2. *J. Biol. Chem.* **1996**, *271*, 33157–33160.
- Marnett, L. J.; Kalgutkar, A. S. Design of Selective Inhibitors of Cyclooxygenase-2 as Nonulcerogenic Anti-Inflammatory Agents. *Curr. Opin. Chem. Biol.* **1998**, *2*, 482–490.
- Vane, J. R. Inhibitors of Prostaglandin Synthesis as a Mechanism of Action for Aspirin-Like Drugs. *Nature (London), New Biol.* **1971**, *231*, 232–235.
- Smith, J. B.; Willis, A. L. Aspirin Selectively Inhibits Prostaglandin Production in Human Platelets. *Nature (London), New Biol.* **1971**, *231*, 235–237.
- Kalgutkar, A. S. Selective Cyclooxygenase-2 Inhibitors as Non-Ulcerogenic Antiinflammatory Agents. *Expert Opin. Ther. Pat.* **1999**, *9*, 831–849.
- DeWitt, D. L. Cox-2-Selective Inhibitors: The New Super Aspirins. *Mol. Pharmacol.* **1999**, *55*, 625–631.
- Vane, J. R.; Botting, R. M. *Clinical Significance and Potential of Selective COX2 Inhibitors*; William Haverly Press: London, 1998.
- Simmons, D. L.; Levy, D. B.; Yannoni, Y.; Erickson, R. L. Identification of a Phorbol Ester-Repressible V-SRC Inducible Gene. *Proc. Natl. Acad. Sci. U.S.A.* **1989**, *86*, 1178–1182.
- Kujubu, D. A.; Fletcher, B. S.; Varnum, B. C.; Lim, R. W.; Herschman, H. R. TIS10, a Phorbol Ester Tumor Promoter-Inducible mRNA from Swiss 3T3 Cells Encodes a Novel Prostaglandin Synthase/Cyclooxygenase Homologue. *J. Biol. Chem.* **1991**, *266*, 12866–12872.
- Xie, W.; Chipman, J. G.; Robertson, D. L.; Erikson, R. L.; Simmons, D. L. Expression of a Mitogen-Responsive Gene Encoding Prostaglandin Synthase Is Regulated by mRNA Splicing. *Proc. Natl. Acad. Sci. U.S.A.* **1991**, *88*, 2692–2696.
- Herschman, H. R. Prostaglandin Synthase 2. *Biochim. Biophys. Acta* **1996**, *1299*, 125–140.
- Hawkey, C. J. COX-2 Inhibitors. *Lancet* **1999**, *353*, 307–314.
- Cohn, S. M.; Schloemann, S.; Tessner, R.; Seibert, K.; Stenson, W. F. Crypt Stem Cell Survival in the Mouse Intestinal Epithelium Is Regulated by Prostaglandins Synthesized through Cyclooxygenase-1. *J. Clin. Invest.* **1997**, *99*, 1367–1379.
- Gans, K. R.; Galbraith, W.; Roman, R. J.; Haber, S. B.; Kerr, J. S.; Schmidt, W. K.; Smith, C.; Hewes, W. E.; Ackerman, N. R. Anti-Inflammatory and Safety Profile of DuP-697, a Novel Orally Effective Prostaglandin Synthesis Inhibitor. *J. Pharmacol. Exp. Ther.* **1990**, *254*, 180–187.
- Seibert, K.; Zhang, Y.; Leahy, K.; Hauser, S.; Masferrer, J.; Perkins, W.; Lee, L.; Isakson, P. Pharmacological and Biochemical Demonstration of the Role of Cyclooxygenase 2 in Inflammation and Pain. *Proc. Natl. Acad. Sci. U.S.A.* **1994**, *91*, 12013–12017.
- Penning, T. D.; Talley, J. J.; Bertenshaw, S. R.; Carter, J. S.; Collins, J. S.; Docter, S.; Graneto, M. J.; Lee, L. F.; Malecha, J. W.; Miyashiro, J. M.; Roger, R. S.; Rogier, D. J.; Yu, S. S.; Anderson, G. D.; Burton, E. G.; Gogburn, J. N.; Gregory, S. A.; Koboldt, C. M.; Perkins, W. E.; Seibert, K.; Veenhizzen, A. W.; Zhang, Y. Y.; Isakson, P. C. Synthesis and Biological Evaluation of the 1,5-Diarylpyrazole Class of Cyclooxygenase-2 Inhibitors: Identification of 4-[5-(4-methylphenyl)-3-(trifluoromethyl)-1H-pyrazol-1-yl]benzenesulfonamide (SC-58635, Celecoxib). *J. Med. Chem.* **1997**, *40*, 1347–1365.
- Prasit, P.; Riendau, D. Selective Cyclooxygenase-2 Inhibitors. In *Annual Reports in Medicinal Chemistry*; Hagmann, W. K., Ed.; Academic Press: San Diego, CA, 1997; Vol. 32, pp 211–220.
- Masferrer, J. L.; Zweifel, B. S.; Manning, P. T.; Hauser, S. D.; Leahy, K. M.; Smith, W. G.; Isakson, P. C.; Seibert, K. Selective Inhibitors of Inducible Cyclooxygenase 2 in Vivo Is Antiinflammatory and Nonulcerogenic. *Proc. Natl. Acad. Sci. U.S.A.* **1994**, *91*, 3228–3232.
- Picot, D.; Loll, P. J.; Garavito, R. M. The X-Ray Crystal Structure of the Membrane Protein Prostaglandin H2 Synthase-1. *Nature* **1994**, *367*, 243–249.
- Kurumbail, R. G.; Stevens, A. M.; Gierse, J. K.; McDonald, J. J.; Stegeman, R. A.; Pak, J. Y.; Dillehaus, D.; Miyashiro, J. M.; Penning, T. D.; Seibert, K.; Isakson, P. C.; Stallings, W. C. Structural Basis for Selective Inhibition of Cyclooxygenase-2 by Antiinflammatory Agents. *Nature* **1996**, *384*, 644–648.
- Habbeeb, A. G.; Rao, P. N. P.; Knaus, E. E. Design and Synthesis of Celecoxib and Rofecoxib Analogues as Selective Cyclooxygenase-2 (COX-2) Inhibitors: Replacement of a Sulfonamide and Methylsulfonyl Pharmacophore by an Azidobioisoster. *J. Med. Chem.* **2001**, *44*, 3039–3042.
- Prasit, P.; Wang, Z.; Brideau, C.; Chan, C. C.; Charleson, S.; Cromlish, W.; Ethier, D.; Evans, J. F.; Ford-Hutchinson, A. W.; Gauthier, J. Y.; Gordon, R.; Guay, J.; Gresser, M.; Kargman, S.; Kennedy, B.; Leblanc, Y.; Léger, S.; Mancini, J.; O'Neill, G. P.; Ouellet, M.; Percival, M. D.; Perrier, H.; Riendeau, D.; Rodger, I.; Tagari, P.; Thérien, M.; Vickers, P.; Wong, E.; Xu, L. J.; Young, R. N.; Zamboni, R. The Discovery of Rofecoxib, [MK966; Vioxx, 4-(4'-methylsulfonylphenyl)-3-phenyl-2(5H)-furanone], an Orally Active Cyclooxygenase-2 Inhibitor. *Bioorg. Med. Chem. Lett.* **1999**, *9*, 1773–1778.
- Talley, J. J.; Brown, D. L.; Carter, J. S.; Graneto, M. J.; Kobolt, C. M.; Masferrer, J. L.; Perkins, W. E.; Roglis, R. S.; Shaffer, A. F.; Zhang, Y. Y.; Zweifel, B. S.; Seibert, K. 4-[5-Methyl-3-phenylisoxazol-4-yl]-benzenesulfonamide, Valdecoxib: A Potent and Selective Inhibitor of COX-2. *J. Med. Chem.* **2000**, *43*, 775–777.
- García-Nieto, R.; Pérez, C.; Gago, F. Automated Docking and Molecular Dynamics Simulations of Nimesulide in the Cyclooxygenase Active Site of Human Prostaglandin-Endoperoxide Synthase-2 (COX-2). *J. Comput.-Aided Mol. Des.* **2000**, *14*, 147–160.
- García-Nieto, R.; Pérez, C.; Checa, A.; Gago, F. Molecular Model of the Interaction between Nimesulide and Human Cyclooxygenase-2. *Rheumatology* **1999**, *38* (Suppl. 1), 14–18.
- Plouffe-Price, M. L.; Jorgensen, W. L. Analysis of Binding Affinities for Celecoxib Analogues with COX-1 and COX-2 from Combined Docking and Monte Carlo Simulations and Insight into the COX-2/COX-1 Selectivity. *J. Am. Chem. Soc.* **2000**, *122*, 9455–9466.
- Wesolowski, S. S.; Jorgensen, W. L. Estimation of Binding Affinities for Celecoxib Analogues with COX-2 via Monte Carlo-Extended Linear Response. *Bioorg. Med. Chem. Lett.* **2002**, *12*, 267–270.
- Chavatte, P.; Yous, S.; Marot, C.; Baurin, N.; Lesieur, D. Three-Dimensional Quantitative Structure–Activity Relationships of Cyclooxygenase-2 (COX-2) Inhibitors: A Comparative Molecular Field Analysis. *J. Med. Chem.* **2001**, *44*, 3223–3330.
- Filizola, M.; Perez, J. J.; Palomer, J. J.; Mauleón, D. Comparative Molecular Modeling Study of the Three-Dimensional Structures of Prostaglandin Endoperoxide H2 Synthase 1 and 2 (COX-1 and COX-2). *J. Mol. Graphics Modell.* **1997**, *15*, 290–300.
- Llorens, O.; Perez, J. J.; Palomer, A.; Mauleón, D. Differential Binding Mode of Diverse Cyclooxygenase Inhibitors. *J. Mol. Graphics Modell.* **2002**, *20*, 359–371.
- Luque, F. J.; Barril, X.; Orozco, M. Fractional Description of Free Energies of Solvation. *J. Comput.-Aided Mol. Des.* **1999**, *13*, 139–152.
- Bachs, M.; Luque, F. J.; Orozco, M. Optimization of Solute Cavities and van der Waals Parameters in Ab Initio MST-SCRF Calculations of Neutral Molecules. *J. Comput. Chem.* **1994**, *15*, 446–454.
- Orozco, M.; Bachs, M.; Luque, F. J. Development of Optimized MST/SCRF Methods for Semiempirical Calculations: The MNDO and PM3 Hamiltonians. *J. Comput. Chem.* **1995**, *16*, 563–575.
- Curutchet, C.; Orozco, M.; Luque, F. J. Solvation in Octanol: Parametrization of the Continuum MST Model. *J. Comput. Chem.* **2001**, *22*, 1180–1193.
- Gelpi, J. L.; Kalko, S. G.; Barril, X.; Cirera, J.; de la Cruz, X.; Luque, F. J.; Orozco, M. Classical Molecular Interaction Potentials: Improved Setup Procedure in Molecular Dynamics Simulations of Proteins. *Proteins* **2001**, *45*, 428.
- Orozco, M.; Luque, F. J. Theoretical Methods for the Description of the Solvent Effect in Biomolecular Systems. *Chem. Rev.* **2000**, *100*, 4187–4225.
- Cornell, W. D.; Cieplak, P.; Bayly, C. I.; Gould, I. R.; Merz, K.; Ferguson, D. M.; Spellmeyer, D. C.; Fox, T.; Caldwell, J. W.; Kollman, P. A. Second Generation Force Field for the Simulation of Proteins, Nucleic Acids, and Organic Molecules. *J. Am. Chem. Soc.* **1995**, *117*, 5179–5197.
- Ryckaert, J. P.; Ciccotti, G.; Berendsen, H. J. C. Numerical Integration of the Cartesian Equations of Motion of a System with Constraints: Molecular Dynamics of *n*-Alkanes. *J. Comput. Phys.* **1977**, *23*, 327–341.
- Jorgensen, W. L.; Chandrasekhar, J.; Madura, J. D.; Impey, R. W.; Klein, M. L. Comparison of Sample Potential Functions for Simulating Liquid Water. *J. Chem. Phys.* **1983**, *79*, 926–935.
- Parameters in AMBER web page were from D. A. Giammona (Ph.D. Thesis, University of California at Davis, 1984).

- (43) Dewar, M. J. S.; Zoebisch, E. G.; Healy, E. F.; Stewart, J. J. P. AM1: A New General Purpose Quantum Mechanical Molecular Model. *J. Am. Chem. Soc.* **1985**, *107*, 3902–3909.
- (44) Bayly, C. I.; Cieplak, P.; Cornell, W. D.; Kollman, P. A. A Well-Behaved Electrostatic Potential Based Method Using Charge Restraints for Deriving Atomic Charges. *J. Chem. Phys.* **1993**, *97*, 10269–10280.
- (45) Aleman, C.; Canela, E. I.; Franco, R.; Orozco, M. A New Strategy for the Evaluation of Force Parameters from Quantum Mechanical Computations. *J. Comput. Chem.* **1991**, *12*, 664–674.
- (46) Kalko, S. G.; Luque, F. J.; Orozco, M. Unpublished version of the UBEXTRACT program, University of Barcelona, 2002.
- (47) Mehler, E. L.; Solmajer, T. Electrostatic Effects in Proteins: Comparison of Dielectric and Charge Models. *Protein Eng.* **1991**, *4*, 903–910.
- (48) Goodsell, D. S.; Olson, A. J. Automated Docking of Substrates to Proteins by Simulated Annealing. *Proteins* **1990**, *8*, 195–202.
- (49) Pearlman, D. A.; Charifson, P. S. Are Free Energy Calculations Useful in Practice? A Comparison with Rapid Scoring Functions for the p38 MAP Kinase Protein System. *J. Med. Chem.* **2001**, *44*, 3417–3423.

JM0209376